Published for SISSA by Springer
Received: December 15, 2015
Accepted: February 6, 2016
Published: March 2, 2016

ε'/ε in 331 models

Andrzej J. Buras[a,b] **and Fulvia De Fazio**[c]

[a] *TUM Institute for Advanced Study, Lichtenbergstr. 2a, D-85747 Garching, Germany*
[b] *Physik Department, Technische Universität München, James-Franck-Straße, D-85747 Garching, Germany*
[c] *Istituto Nazionale di Fisica Nucleare, Sezione di Bari, Via Orabona 4, I-70126 Bari, Italy*

E-mail: andrzej.buras@tum.de, fulvia.defazio@ba.infn.it

Abstract: Motivated by the recent findings that the ratio ε'/ε in the Standard Model (SM) appears to be significantly below the data we investigate whether the necessary enhancement of ε'/ε can be obtained in 331 models, based on the gauge group $\mathrm{SU}(3)_C \times \mathrm{SU}(3)_L \times \mathrm{U}(1)_X$. In these models new physics (NP) contributions to ε'/ε and other flavour observables are dominated by tree-level exchanges of a Z' with non-negligible contributions from tree-level Z exchanges generated through the $Z - Z'$ mixing. NP contributions to ε'/ε in these models are governed by the electroweak penguin operator Q_8 for which the hadronic matrix element is already rather well known so that our analysis of NP contributions is subject to much smaller theoretical uncertainties than within the SM. In particular strong cancelations between different contributions do not take place. The size of NP effects depends not only on $M_{Z'}$ but in particular on a parameter β, which distinguishes between various 331 models. Also a parameter $\tan\bar{\beta}$ present in the $Z - Z'$ mixing plays a role. We perform the analysis in seven 331 models characterized by different β, $\tan\bar{\beta}$ and fermion representations under the gauge group that have been selected in our earlier analysis on the basis of electroweak precision data. Imposing the constraints from $\Delta F = 2$ transitions we find that only three of these models can provide a significant positive shift in ε'/ε up to 6×10^{-4} for $M_{Z'} = 3\,\mathrm{TeV}$. Two of them allow simultaneously a supression of the rate for $B_s \to \mu^+\mu^-$ by 20% thereby bringing the theory closer to the data without any significant impact on the Wilson coefficient C_9. The third model provides simultaneous shift $\Delta C_9 = -0.6$, softening the anomalies in $B \to K^*\mu^+\mu^-$, without any significant impact on $B_s \to \mu^+\mu^-$. NP effects in rare K decays, in particular in $K^+ \to \pi^+\nu\bar{\nu}$, turn out to be small. This is also the case of $B \to K(K^*)\nu\bar{\nu}$. Both predictions could be challenged by NA62 experiment and Belle II in this decade. The special flavour structure of 331 models implies that even for $M_{Z'} = 30\,\mathrm{TeV}$ a shift of ε'/ε up to 8×10^{-4} and a significant shift in ε_K can be obtained, while the effects in other flavour observables are small. In this manner ε'/ε and ε_K appear to be unique flavour observables in these models which provide the possibility of accessing masses of $M_{Z'}$ far beyond the LHC reach.

Keywords: Beyond Standard Model, Heavy Quark Physics, CP violation, Kaon Physics

ArXiv ePrint: 1512.02869v2

doi:10.1007/JHEP03(2016)010

JHEP03(2016)010

Contents

1 Introduction **1**

2 Basic formula for ε'/ε in 331 Models **4**
- 2.1 Preliminaries 4
- 2.2 Z' contribution 5
- 2.3 Z contribution 6
- 2.4 Final formula 7

3 Implications of enhanced ε'/ε in 331 models **7**
- 3.1 Favourite 331 models 7
- 3.2 Predictions for ε'/ε in favourite models 9

4 Z' outside the reach of the LHC **15**

5 Summary **20**

1 Introduction

The recent findings that the ratio ε'/ε predicted by the Standard Model (SM) appears to be significantly below the experimental data [1] poses a natural question what kind of new physics (NP) could be responsible for this new anomaly. In the present paper we will address this question in 331 models based on the gauge group $\mathrm{SU}(3)_C \times \mathrm{SU}(3)_L \times \mathrm{U}(1)_X$ [2, 3]. These models display several appealing features. The first one is that the requirement of asymptotic freedom of QCD together with that of anomaly cancelation constrains the number of generations to be necessarily equal to the number of colours, providing an explanation for the existence of three generations. Moreover, under the action of $\mathrm{SU}(3)_L$ two quark generations should transform as triplets, one as an antitriplet. Adopting the choice that the third generation is the one transforming as an antitriplet, this different treatment could be at the origin of the large top mass. It should be recalled that some of the generators of the group are connected by the relation $Q = T_3 + \beta T_8 + X$ where Q is the electric charge, T_3 and T_8 are two of the SU(3) generators and X the generator of $\mathrm{U}(1)_X$. β is a parameter that defines a specific variant of the model.

Several new particles are present in these models, their features depending on the chosen variant. However, in all the variants a new neutral gauge boson Z' exists that can mediate tree level flavour changing neutral currents (FCNC) in the quark sector.

In the framework of 331 models, the ratio ε'/ε has been studied in our earlier analysis [4]. Here we update it and improve it.

JHEP03(2016)010

Recent analyses addressing the implications of new value of ε'/ε within the SM for NP in the Littlest Higgs model with T-parity and simplified Z and Z' models can be found in [5] and [6], respectively.

The present status of ε'/ε in the SM has been reviewed recently in [1], where references to rich literature can be found. After the new results for the hadronic matrix elements of QCD penguin and electroweak penguin $(V-A)\otimes(V+A)$ operators from RBC-UKQCD lattice collaboration [7, 8] and the extraction of the corresponding matrix elements of penguin $(V-A)\otimes(V-A)$ operators from the CP-conserving $K\to\pi\pi$ amplitudes one finds [1]

$$\varepsilon'/\varepsilon = (1.9 \pm 4.5)\times 10^{-4}\,. \tag{1.1}$$

This result differs with $2.9\,\sigma$ significance from the experimental world average from NA48 [9] and KTeV [10, 11] collaborations,

$$(\varepsilon'/\varepsilon)_{\rm exp} = (16.6 \pm 2.3)\times 10^{-4}\,, \tag{1.2}$$

suggesting evidence for NP in K decays.

But even discarding the lattice results and using instead newly derived upper bounds on the matrix elements of the dominant penguin operators from large N approach [12], one finds at most [1]

$$(\varepsilon'/\varepsilon)_{\rm SM} = (8.6 \pm 3.2)\times 10^{-4}\,, \tag{1.3}$$

still $2\,\sigma$ below the experimental data.

The dominant uncertainty in the SM prediction for ε'/ε originates from the partial cancellation between QCD penguin contributions and electroweak penguin contributions that depend sensitively on the parameters $B_6^{(1/2)}$ and $B_8^{(3/2)}$, respectively. QCD penguins give a positive contribution while electroweak penguins a negative one. Fortunately a new insight in the values of these parameters has been obtained recently through the results from the RBC-UKQCD collaboration on the relevant hadronic matrix elements of the operators Q_6 [8] and Q_8 [7] and upper bounds on both $B_6^{(1/2)}$ and $B_8^{(3/2)}$ which can be derived from large N approach [12].

The results from the RBC-UKQCD collaboration imply the following values for $B_6^{(1/2)}$ and $B_8^{(3/2)}$ [1, 13]

$$B_6^{(1/2)} = 0.57 \pm 0.19\,, \qquad B_8^{(3/2)} = 0.76 \pm 0.05\,, \qquad \text{(RBC-UKQCD)} \tag{1.4}$$

and the bounds from large N approach read [12]

$$B_6^{(1/2)} \le B_8^{(3/2)} < 1 \qquad \text{(large-}N\text{)}. \tag{1.5}$$

While one finds in this approach $B_8^{(3/2)}(m_c) = 0.80 \pm 0.10$, the result for $B_6^{(1/2)}$ is less precise but there is a strong indication that $B_6^{(1/2)} < B_8^{(3/2)}$ in agreement with (1.4). For further details, see [12].

In 331 models we have

$$\left(\frac{\varepsilon'}{\varepsilon}\right)_{331} = \left(\frac{\varepsilon'}{\varepsilon}\right)_{\rm SM} + \left(\frac{\varepsilon'}{\varepsilon}\right)_{Z'} + \left(\frac{\varepsilon'}{\varepsilon}\right)_{Z} \equiv \left(\frac{\varepsilon'}{\varepsilon}\right)_{\rm SM} + \Delta(\varepsilon'/\varepsilon) \tag{1.6}$$

JHEP03(2016)010

with the $\Delta(\varepsilon'/\varepsilon)$ resulting from tree-level Z' and Z exchanges. In this paper we will concentrate exclusively on this shift in ε'/ε, which as we will see has significantly smaller theoretical uncertainties than the SM part.

Indeed, as demonstrated by us in [4], the shift in ε'/ε in question is in 331 models governed by the electroweak $(V-A)\times(V+A)$ penguin operator

$$Q_8 = \frac{3}{2}\,(\bar{s}_\alpha d_\beta)_{V-A} \sum_{q=u,d,s,c,b,t} e_q\,(\bar{q}_\beta q_\alpha)_{V+A} \tag{1.7}$$

with only small contributions of other operators that we will neglect in what follows.

As the relevant non-perturbative parameter $B_8^{(3/2)}$ is much better known than $B_6^{(1/2)}$, the non-perturbative uncertainty in NP contributions in (1.6) is significantly smaller than in the SM term. Moreover, except for the value of $B_8^{(3/2)}$, the NP contributions are fully independent from the SM one. Consequently we can fully concentrate on the these new contributions and investigate which 331 models can bring theory closer to data. It will also be interesting to see what this implies for other flavour observables, in particular branching ratios for $B_{s,d}\to\mu^+\mu^-$, $B\to K(K^*)\nu\bar{\nu}$, $K^+\to\pi^+\nu\bar{\nu}$, $K_L\to\pi^0\nu\bar{\nu}$ and the Wilson coefficient C_9 that enters the discussion of $B\to K^*\mu^+\mu^-$ anomalies.

In this context our detailed analyses of FCNC processes in 331 models in [14, 15] will turn out to be useful. References to earlier analysis of flavour physics in 331 models can be found there and in [16, 17]. But the ratio ε'/ε has been analyzed in 331 models only in [4]. However, in that paper values of $B_6^{(1/2)}$ as high as 1.25 and thus violating the bounds in (1.5) have been considered. As seen in figure 14 of that paper in this case the resulting ε'/ε in the SM can even be larger than the data so that dependently on the chosen value of $B_6^{(1/2)}$ both enhancements and suppressions of ε'/ε in a given model were required to fit the data in (1.2) with different implications for $K_L\to\pi^0\nu\bar{\nu}$. With the new results in (1.4) and (1.5) the situation changed drastically and one needs a significant enhancement relative to the SM prediction.

The main new aspects of the present paper relative to [4] are as follows:

- We update our analysis of $\Delta(\varepsilon'/\varepsilon)$ by taking new result on $B_8^{(3/2)}$ into account. We also include in the discussion second fermion representation (F_2) which was not considered by us in the context of ε'/ε previously.

- After the constraints from $\Delta F=2$ transitions have been taken into account the size of the possible enhancement of ε'/ε depends on a given model and in certain models it is too small to be relevant. Such models are then disfavoured.

- Further selection of the models is provided through the correlation of ε'/ε with other flavour observables, in particular the decays $B_s\to\mu^+\mu^-$, $B\to K^*\mu^+\mu^-$, $K_L\to\pi^0\nu\bar{\nu}$, $K^+\to\pi^+\nu\bar{\nu}$ and $B\to K(K^*)\nu\bar{\nu}$. While a definite selection is not possible at present, because the data is not sufficiently precise, it will be possible in the coming years.

In [4] we have considered several 331 models corresponding to four different values of β, three values of $\tan\bar{\beta}$ related to $Z-Z'$ mixing and two fermion representations F_1 and

JHEP03(2016)010

F_2. 24 models in total. Among them 7 have been favoured by electroweak precision tests and we will concentrate our analysis on them. The important result of the present paper is that the requirement of significant enhancement of ε'/ε reduces the number of favourite models to 3.

Our paper is organized as follows. In section 2 we present the general formula for ε'/ε in 331 models which is now valid for both fermion representations considered in [4]. In section 3 we first briefly introduce the 7 favourite 331 models that have been selected in [4] on the basis of electroweak precision data. Subsequently, imposing the constraints from $\Delta F = 2$ transitions in K and $B_{s,d}$ systems, we find that only three models are of interest for ε'/ε. Subsequently we demonstrate that the correlations of $\Delta(\varepsilon'/\varepsilon)$ with rare decays in these three models can provide further selection between them when the data on flavour observables considered by us improves. In section 4 we consider the case of a Z' outside the reach of the LHC. The particular flavour structure of 331 models implies that for $M_{Z'} \geq 10\,\text{TeV}$, NP effects in rare $B_{s,d}$ decays, $K^+ \to \pi^+\nu\bar{\nu}$ and $K_L \to \pi^0\nu\bar{\nu}$ are very small, while the ones in ϵ_K and ε'/ε can be significant even for $M_{Z'} = 30\,\text{TeV}$. We conclude in section 5. Except for the formulae for ε'/ε, all other expressions for observables considered by us can be found in [4, 14, 15] and we will not repeat them here. But in table 3 we give all relevant input parameters which occassionaly differ from the ones used in [4, 14, 15].

2 Basic formula for ε'/ε in 331 Models

2.1 Preliminaries

In 331 models ε'/ε receives the dominant new contribution from tree-level Z' exchanges but through $Z - Z'$ mixing, analyzed in detail in [4], contributions from tree-level Z exchanges in certain models and for certain values of new parameters cannot be neglected. We begin with general expressions valid for both Z' and Z contributions which will allow us to recall all the relevant parameters of the 331 models. Subsequently we will specify these expressions to Z' and Z cases which differ only by the value of the Wilson coefficient of the Q_8 operator at the low renormalization scale at which the relevant hadronic matrix element of Q_8 is calculated.

The basic expression for $V = (Z', Z)$ contribution to ε'/ε is given by

$$\left(\frac{\varepsilon'}{\varepsilon}\right)_V = \frac{\omega}{|\varepsilon_K|\sqrt{2}} \frac{\text{Im}A_2(V)}{\text{Re}A_2}, \qquad \omega = \frac{\text{Re}A_2}{\text{Re}A_0} = (4.46) \times 10^{-2}\,. \tag{2.1}$$

The factor ω differs by 10% from the corresponding factor ω_+ in [4] as discussed in [1].

In evaluating (2.1) we use, as in the case of the SM, the experimental values for $\text{Re}A_2$ and ε_K:

$$\text{Re}A_2 = 1.210(2) \times 10^{-8}\ \text{GeV}, \qquad |\varepsilon_K| = 2.228(11) \times 10^{-3}\,. \tag{2.2}$$

The amplitude $A_2(V)$ is dominated by the contribution of the Q_8 operator and is given by

$$A_2(V) = C_8(m_c, V)\langle Q_8(m_c)\rangle_2 \tag{2.3}$$

with $C_8(m_c, V)$ given below.

The hadronic matrix element is given by

$$\langle Q_8(m_c)\rangle_2 = \sqrt{2}\left[\frac{m_{\rm K}^2}{m_s(m_c)+m_d(m_c)}\right]^2 F_\pi\, B_8^{(3/2)} = 0.862\, B_8^{(3/2)}\ {\rm GeV}^3. \tag{2.4}$$

The normalization of our amplitudes is such that $\langle Q_8(m_c)\rangle_2$ is by a factor of $\sqrt{\frac{3}{2}}$ smaller than the one in [1]. Correspondingly the value of ${\rm Re}A_2$ in (2.2) is by this factor smaller than in [1]. The choice of the scale $\mu = m_c$ is convenient as it is used in analytic formulae for ε'/ε in [1]. In our numerical calculations we will use $B_8^{(3/2)} = 0.76$ and the values [18, 19]

$$m_K = 497.614\,{\rm MeV}, \qquad F_\pi = 130.41(20)\,{\rm MeV}, \qquad \frac{F_K}{F_\pi} = 1.194(5)\,, \tag{2.5}$$

$$m_s(m_c) = 109.1(2.8)\,{\rm MeV}, \qquad m_d(m_c) = 5.44(19)\,{\rm MeV}\,. \tag{2.6}$$

New sources of flavour and CP violation in 331 models are parametrized by new mixing parameters and phases

$$\tilde{s}_{13}, \qquad \tilde{s}_{23}, \qquad \delta_1, \qquad \delta_2 \tag{2.7}$$

with $\tilde{s}_{13}$ and $\tilde{s}_{23}$ positive definite and $0 \le \delta_{1,2} \le 2\pi$. They can be constrained by flavour observables as demonstrated in detail in [14].

Noticeably, constraints deriving from $\Delta F = 2$ observables do not depend on the choice of the fermion representation. We recall here that, as already mentioned, the choice of the transformation properties of the fermions under the gauge group of 331 models, and in particular under the action of ${\rm SU}(3)_L$, is not unique. Following [4] we denote by F_1 the fermion representation in which the first two generations of quarks transform as triplets under ${\rm SU}(3)_L$ while the third one as well as leptons transform as antitriplets. On the other hand, F_2 corresponds to the case in which the choice of triplets and antitriplets is reversed. Right-handed fermions are always singlets.

2.2 Z' contribution

For the fermion representation F_1 we find

$$C_8(m_c, Z') = 1.35\left[\frac{g_2 s_W^2}{6c_W}\right]_{M_{Z'}} \beta\sqrt{f(\beta)}\frac{\Delta_L^{sd}(Z')}{M_{Z'}^2} = 4.09\times 10^{-2}\beta\sqrt{f(\beta)}\frac{\Delta_L^{sd}(Z')}{M_{Z'}^2} \tag{2.8}$$

with 1.35 being renormalization group factor calculated for $M_{Z'} = 3\,{\rm TeV}$ in [4]. $C_8(m_c, Z')$ depends through $\beta\sqrt{f(\beta)}$ on the 331 model considered where

$$f(\beta) = \frac{1}{1-(1+\beta^2)s_W^2} > 0\,. \tag{2.9}$$

We have indicated that the values of g_2 and s_W^2 should be evaluated at $M_{Z'}$ with $s_W^2 = \sin^2\theta_W = 0.249$ and $g_2(M_{Z'}) = 0.633$ corresponding to $M_{Z'} = 3\,{\rm TeV}$.

The coupling $\Delta_L^{sd}(Z')$ is given in terms of the parameters in (2.7) as follows

$$\Delta_L^{sd}(Z') = \frac{g_2(M_{Z'})}{\sqrt{3}} c_W \sqrt{f(\beta)}\tilde{s}_{13}\tilde{s}_{23}e^{i(\delta_2-\delta_1)}\,. \tag{2.10}$$

The formulae (2.8)–(2.10) are valid for the fermion representation F_1. For a given β, the formulae for the fermion representation F_2 are obtained by reversing the sign in front of β. We note that $\Delta_L^{sd}(Z')$ is independent of the fermion representation as $f(\beta)$ depends only on β^2.

Combining all these formulae we find

$$\left(\frac{\varepsilon'}{\varepsilon}\right)_{Z'} = \pm 1.10\,[\beta f(\beta)]\,\tilde{s}_{13}\tilde{s}_{23}\sin(\delta_2-\delta_1)\left[\frac{B_8^{(3/2)}}{0.76}\right]\left[\frac{3\,\text{TeV}}{M_{Z'}}\right]^2 \tag{2.11}$$

with the upper sign for F_1 and the lower for F_2

We observe that the contribution of Z' to ε'/ε is invariant under the transformation

$$\beta \to -\beta, \qquad F_1 \to F_2\,. \tag{2.12}$$

This invariance is in fact valid for other flavour observables in the absence of $Z-Z'$ mixing. But as pointed out in [4] in the presence of this mixing it is broken as we will see soon.

2.3 Z contribution

In the case of tree-level Z contribution also the operator Q_8 dominates but its Wilson coefficient is given first by [20]

$$C_8(m_c,Z) = -0.76\left[\frac{g_2 s_W^2}{6c_W}\right]_{M_Z}\frac{\Delta_L^{sd}(Z)}{M_Z^2}\,. \tag{2.13}$$

Here $g_2 = g_2(M_Z) = 0.652$ is the $\text{SU}(2)_L$ gauge coupling and the factor 0.76 is the outcome of the RG evolution.

In the 331 models the flavour violating couplings of Z are generated through $Z-Z'$ mixing. They are given by [4]

$$\Delta_L^{ij}(Z) = \sin\xi\,\Delta_L^{ij}(Z') \qquad (i\neq j) \tag{2.14}$$

with

$$\sin\xi = \frac{c_W^2}{3}\sqrt{f(\beta)}\left(3\beta\frac{s_W^2}{c_W^2}+\sqrt{3}a\right)\left[\frac{M_Z^2}{M_{Z'}^2}\right] \equiv B(\beta,a)\left[\frac{M_Z^2}{M_{Z'}^2}\right] \tag{2.15}$$

describing the $Z-Z'$ mixing, where $s_W^2 = 0.23126$. It should be stressed that this mixing is independent of the fermion representation. Here

$$a = \frac{1-\tan^2\bar{\beta}}{1+\tan^2\bar{\beta}}, \qquad \tan\bar{\beta} = \frac{v_\rho}{v_\eta}. \tag{2.16}$$

As the vacuum expectation values of the Higgs triplets ρ and η are responsible for the masses of up-quarks and down-quarks, respectively, we expressed the parameter a in terms of the usual $\tan\bar{\beta}$ where we introduced a *bar* to distinguish the usual angle β from the parameter β in 331 models. See [4] for further details.

We thus find

$$C_8(m_c,Z) = -0.76\left[\frac{g_2 s_W^2}{6c_W}\right]_{M_Z}B(\beta,a)\frac{\Delta_L^{sd}(Z')}{M_{Z'}^2}\,. \tag{2.17}$$

β	$-\frac{2}{\sqrt{3}}$	$-\frac{1}{\sqrt{3}}$	$\frac{1}{\sqrt{3}}$	$\frac{2}{\sqrt{3}}$
$R_{\varepsilon'}$ $(\tan\bar{\beta}=0.2)$	± 0.066	± 0.25	∓ 0.50	∓ 0.31
$R_{\varepsilon'}$ $(\tan\bar{\beta}=1.0)$	∓ 0.12	∓ 0.12	∓ 0.12	∓ 0.12
$R_{\varepsilon'}$ $(\tan\bar{\beta}=5.0)$	∓ 0.31	∓ 0.50	± 0.25	± 0.066

Table 1. $R_{\varepsilon'}$ for different β and $\tan\bar{\beta}$. The upper sign is for F_1, the lower for F_2.

Combining these formulae allows to derive a simple relation

$$\left(\frac{\varepsilon'}{\varepsilon}\right)_Z = R_{\varepsilon'}\left(\frac{\varepsilon'}{\varepsilon}\right)_{Z'}, \tag{2.18}$$

where

$$R_{\varepsilon'} = \frac{C_8(m_c,Z)}{C_8(m_c,Z')} = \mp\frac{0.53}{\beta}\,\frac{c_W^2}{3}\left[3\beta\frac{s_W^2}{c_W^2}+\sqrt{3}a\right]. \tag{2.19}$$

The upper sign in the expression (2.19) is valid for fermion representation F_1, the lower for F_2. The values of $R_{\varepsilon'}$ are listed in table 1 for various values of β, $\tan\bar{\beta}$ and the representations F_1 and F_2. Evidently Z' dominates NP contributions to ε'/ε implying that $Z-Z'$ mixing effects are small in this ratio. The two exceptions are the case of $\beta=-1/\sqrt{3}$ and $\tan\bar{\beta}=5$ and the case of $\beta=1/\sqrt{3}$ and $\tan\bar{\beta}=0.2$ for which Z contribution reaches 50% of the Z' one. However, as seen in table 2 both models are not among favourits and the largest $Z-Z'$ effect of 25% among the chosen models in that table is found in M6.

It should be noted that whereas the Z' contribution to ε'/ε for the representation F_2 differs from the one for F_1 by sign, the contribution of Z to ε'/ε is independent of the fermion representation. This disparity breaks the invariance in (2.12). Analogous feature is observed in several other flavour observables.

2.4 Final formula

The final expression for the shift of ε'/ε in 331 models is given by

$$\Delta(\varepsilon'/\varepsilon) = (1+R_{\varepsilon'})\left(\frac{\varepsilon'}{\varepsilon}\right)_{Z'}. \tag{2.20}$$

In the next section we will investigate, which 331 models can provide a significant shift $\Delta(\varepsilon'/\varepsilon)$ for $M_{Z'}=3\,\text{TeV}$ and how this shift is correlated with other flavour observables.

3 Implications of enhanced ε'/ε in 331 models

3.1 Favourite 331 models

The favourite 331 models selected in [4] on the basis of their perfomance in electroweak precision tests are listed in the notation of that paper in table 2. In addition to the fermion representation and the values of β and $\tan\bar{\beta}$ in a given model we indicate how in that model NP effects in the branching ratio for $B_s\to\mu^+\mu^-$ are correlated with the ones in C_9. For $\mathcal{B}(B_s\to\mu^+\mu^-)$ the signs $\pm$ denote the enhancement and suppression of it with

MI	scen.	β	$\tan\bar{\beta}$	$\mathcal{B}(B_s \to \mu^+\mu^-)$	C_9	$\sin(\delta_2 - \delta_1)$
M3	F_1	$-1/\sqrt{3}$	1	$\pm$	$\pm$	-1
M6	F_1	$1/\sqrt{3}$	5	$\pm$	0	$+1$
M8	F_1	$2/\sqrt{3}$	5	$\pm$	$\mp$	$+1$
M9	F_2	$-2/\sqrt{3}$	1	$\pm$	$\mp$	$+1$
M11	F_2	$-1/\sqrt{3}$	1	$\pm$	0	$+1$
M14	F_2	$1/\sqrt{3}$	5	$\pm$	$\pm$	-1
M16	F_2	$2/\sqrt{3}$	5	$\pm$	$\pm$	-1

Table 2. Definition of the favourite 331 models. See text for explanation of the columns for $B_s \to \mu^+\mu^-$ and C_9. In the last column we list the values of $\sin(\delta_2 - \delta_1)$ for which the maximal *positive* shifts of ε'/ε in a given model can be obtained.

respect to its SM value, respectively. C_9 in the SM is positive and $\pm$ also here denote the enhancements and suppressions with respect to its SM value, respectively. In M6 and M11 NP contributions to C_9 are fully negligible. These correlations are shown in figure 15 of [4].

Before entering the discussion of ε'/ε let us recall that the present data favour simultaneous suppressions of $\mathcal{B}(B_s \to \mu^+\mu^-)$ and C_9. From figure 15 in [4] and table 2 we reach the following conclusions.

- Qualitatively models M3, M14 and M16 can provide simultaneous suppression of $\mathcal{B}(B_s \to \mu^+\mu^-)$ and a negative shift $\mathrm{Re}C_9^{\mathrm{NP}}$ but the suppression of $\mathcal{B}(B_s \to \mu^+\mu^-)$ is not significant.

- For softening the $B_d \to K^*\mu^+\mu^-$ anomaly the most interesting is the model M16. If the anomaly in question remains but decreases with time also models M3 and M14 would be of interest.

- The remaining four models, in fact the four top models on our list of favourites in (3.1) below, as far as electroweak precision tests are concerned, do not provide any explanation of $B_d \to K^*\mu^+\mu^-$ anomaly but are interesting for $B_s \to \mu^+\mu^-$ decay. These are M6, M8, M9 and M11, the first two with F_1 and the last two with F_2 fermion representation. It turns out that the strongest suppression of the rate for $B_s \to \mu^+\mu^-$ can be achieved in M8 and M9. In fact these two models are the two leaders on the list of favourites in (3.1). But in these models C_9 is enhanced and not suppressed as presently observed in the data. The suppression of the $B_s \to \mu^+\mu^-$ rate is smaller in M6 and M11 but there the shift in C_9 can be neglected.

We conclude that when the data for $\mathcal{B}(B_s \to \mu^+\mu^-)$ and C_9 improve we will be able to reduce the number of favourite models. But if both will be significantly suppressed none of the models considered here will be able to describe the data. In fact model M2 with F_1, $\beta = -2/\sqrt{3}$ and $\tan\bar{\beta} = 5$ could in principle do this work here but it is disfavoured through electroweak precision tests.

JHEP03(2016)010

Concerning these tests the ranking is given as follows

$$\text{M9}, \quad \text{M8}, \quad \text{M6}, \quad \text{M11}, \quad \text{M3}, \quad \text{M16}, \quad \text{M14}, \qquad \text{(favoured)} \tag{3.1}$$

with the first five performing better than the SM while the last two basically as the SM. The models with *odd* index I correspond to $\tan\bar{\beta} = 1.0$ and the ones with *even* one to $\tan\bar{\beta} = 5.0$. None of the models with $\tan\bar{\beta} = 0.2$ made this list implying reduced impact of $Z - Z'$ mixing on ε'/ε and small NP effects in decays with neutrinos in the final state.

3.2 Predictions for ε'/ε in favourite models

After the recollection of the correlations among B physics observables in the seven models in questions we are in the position to investigate which of these models allow for significant enhancement of ε'/ε.

To this end we set the CKM parameters to

$$|V_{ub}| = 3.6 \times 10^{-3}, \qquad |V_{cb}| = 42.0 \times 10^{-3}, \qquad \gamma = 70^\circ. \tag{3.2}$$

This choice is in the ballpark of present best values for these three parameters but is also motivated by the fact that NP contributions to ε_K in 331 models are rather small for $M_{Z'}$ of a few TeV and SM should perform well in this case. Indeed for this choice of CKM parameters we find

$$|\varepsilon_K|_{\rm SM} = 2.14 \times 10^{-3}, \qquad (\Delta M_K)_{\rm SM} = 0.467 \cdot 10^{-2}\,{\rm ps}^{-1} \tag{3.3}$$

and $|\varepsilon_K|$ in the SM only 4% below the data. Due to the presence of long distance effects in ΔM_K also this value is compatible with the data. Moreover, the resulting ${\rm Im}\lambda_t = 1.42 \times 10^{-4}$ is very close to the central value ${\rm Im}\lambda_t = 1.40 \times 10^{-4}$ used in [1]. While our choice of CKM parameters is irrelevant for the shift in ε'/ε it matters in the predictions for NP contributions to rare K and B decays due to the their intereference with SM contributions.

Next, as in [14], we perform a simplified analysis of $\Delta M_{d,s}$, $S_{\psi K_S}$ and $S_{\psi\phi}$ in order to identify oases in the space of four parameters in (2.7) for which these four observables are consistent with experiment. To this end we use the formulae for $\Delta F = 2$ observables in [4, 14] and set all input parameters listed in table 3 at their central values. But in order to take partially hadronic and experimental uncertainties into account we require the 331 models to reproduce the data for $\Delta M_{s,d}$ within $\pm 10\%(\pm 5\%)$ and the data on $S_{\psi K_S}$ and $S_{\psi\phi}$ within experimental 2σ. As seen in table 3 the present uncertainties in hadronic parameters relevant for $\Delta M_{s,d}$ are larger than 10% but we anticipate progress in the coming years. The accuracy of $\pm 5\%$ should be achieved at the end of this decade.

Specifically, our search is governed by the following allowed ranges:

$$16.0\,(16.9)/{\rm ps} \le \Delta M_s \le 19.5\,(18.7)/{\rm ps}, \quad -0.055 \le S_{\psi\phi} \le 0.085, \tag{3.4}$$

$$0.46\,(0.48)/{\rm ps} \le \Delta M_d \le 0.56\,(0.53)/{\rm ps}, \quad 0.657 \le S_{\psi K_S} \le 0.725\,, \tag{3.5}$$

JHEP03(2016)010

$G_F = 1.16638(1) \cdot 10^{-5}\,\text{GeV}^{-2}$	[18]	$m_{B_d} = 5279.58(17)\,\text{MeV}$	[18]
$M_W = 80.385(15)\,\text{GeV}$	[18]	$m_{B_s} = 5366.8(2)\,\text{MeV}$	[18]
$\sin^2\theta_W = 0.23126(13)$	[18]	$F_{B_d} = 190.5(42)\,\text{MeV}$	[19]
$\alpha(M_Z) = 1/127.9$	[18]	$F_{B_s} = 227.7(45)\,\text{MeV}$	[19]
$\alpha_s(M_Z) = 0.1185(6)$	[18]	$\hat{B}_{B_d} = 1.27(10)$, $\hat{B}_{B_s} = 1.33(6)$	[19]
$m_d(2\,\text{GeV}) = 4.68(16)\,\text{MeV}$	[19]	$\hat{B}_{B_s}/\hat{B}_{B_d} = 1.06(11)$	[19]
$m_s(2\,\text{GeV}) = 93.8(24)\,\text{MeV}$	[19]	$F_{B_d}\sqrt{\hat{B}_{B_d}} = 216(15)\,\text{MeV}$	[19]
$m_c(m_c) = 1.275(25)\,\text{GeV}$	[18]	$F_{B_s}\sqrt{\hat{B}_{B_s}} = 266(18)\,\text{MeV}$	[19]
$m_b(m_b) = 4.18(3)\,\text{GeV}$	[18]	$\xi = 1.268(63)$	[19]
$m_t(m_t) = 163(1)\,\text{GeV}$	[21]	$\eta_B = 0.55(1)$	[22, 23]
$m_K = 497.614(24)\,\text{MeV}$	[18]	$\Delta M_d = 0.510(3)\,\text{ps}^{-1}$	[24]
$F_K/F_\pi = 1.194(5)$	[18]	$\Delta M_s = 17.757(21)\,\text{ps}^{-1}$	[24]
$F_\pi = 130.41(20)\,\text{MeV}$	[18]	$S_{\psi K_S} = 0.691(17)$	[24]
$\hat{B}_K = 0.750(15)$	[19, 25]	$S_{\psi\phi} = 0.015(35)$	[24]
$\kappa_\epsilon = 0.94(2)$	[26, 27]	$\Delta\Gamma_s/\Gamma_s = 0.122(9)$	[24]
$\eta_{cc} = 1.87(76)$	[28]	$\tau_{B_s} = 1.509(4)\,\text{ps}$	[24]
$\eta_{tt} = 0.5765(65)$	[22]	$\tau_{B_d} = 1.520(4)\,\text{ps}$	[24]
$\eta_{ct} = 0.496(47)$	[29]	$\tau_{B^\pm} = 1.638(4)\,\text{ps}$	[24]
$\Delta M_K = 0.5293(9) \cdot 10^{-2}\,\text{ps}^{-1}$	[18]	$\lvert V_{us}\rvert = 0.2253(8)$	[18]
$\lvert\epsilon_K\rvert = 2.228(11) \cdot 10^{-3}$	[18]	$\gamma = (73.2^{+6.3}_{-7.0})^\circ$	[30]

Table 3. Values of the experimental and theoretical quantities used as input parameters as of June 2015. For future updates see PDG [18], FLAG [19] and HFAG [24].

where the values in parentheses correspond to decreased uncertainty. For the central parameters we find in the SM

$$(\Delta M_s)_{\text{SM}} = 18.45/\text{ps}, \quad (\Delta M_d)_{\text{SM}} = 0.558/\text{ps}, \quad S^{\text{SM}}_{\psi\phi} = 0.037, \quad S^{\text{SM}}_{\psi K_S} = 0.688\,. \tag{3.6}$$

In the case of ε_K the status of hadronic parameters is better than for $\Delta M_{s,d}$ but the CKM uncertainties are larger and the result depends on whether inclusive or exclusive determinations of $|V_{ub}|$ and $|V_{cb}|$ are used. As we keep these parameters fixed we include this uncertainty by choosing the allowed range for $|\varepsilon_K|$ below to be roughly the range one would get in the SM by varying $|V_{ub}|$ and $|V_{cb}|$ in their ranges known from tree-level determinations.

The uncertainties in ΔM_K are very large both due to the presence of long distance effects and large uncertainty in η_{cc}. We could in principle ignore this constraint but as we will see in the next section it plays a role for $M_{Z'}$ above 30 TeV not allowing for large shifts in ε'/ε in 331 models for such high values of $M_{Z'}$. In fact as we will explain in the next section it is ΔM_K and not ε_K which is most constraining the maximal values of ε'/ε.

JHEP03(2016)010

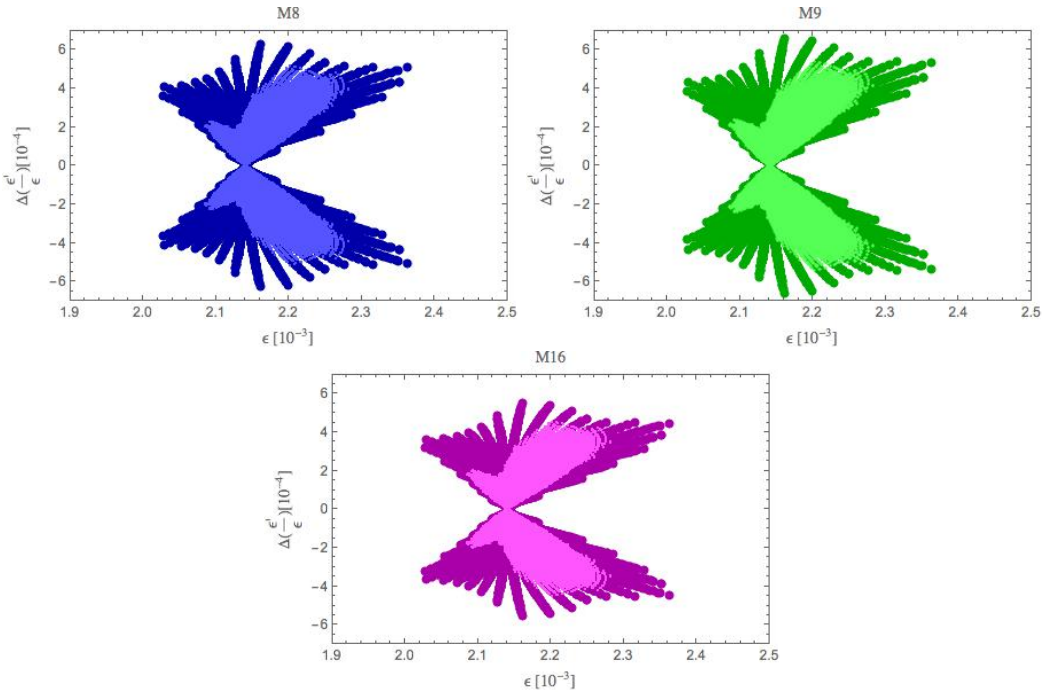

Figure 1. $\Delta(\varepsilon'/\varepsilon)$ versus ε_K for M8, M9 and M16. $M_{Z'} = 3\,\text{TeV}$. Darker regions correspond to present constraints on $\Delta M_{s,d}$ and lighter ones to future projection.

But at the LHC scales and even at $M_{Z'} = 10\,\text{TeV}$ the ΔM_K constraint is irrelevant. Only for scales above $M_{Z'} = 30\,\text{TeV}$ it starts to play an important role bounding the maximal values of ε'/ε. Once the knowledge of long distance effects improves and the error on η_{cc} decreases it will be possible to improve our analysis in this part.

We will then impose the ranges

$$1.60 \times 10^{-3} < |\varepsilon_K| < 2.50 \times 10^{-3}\,, \qquad -0.30 \le \frac{(\Delta M_K)^{Z'}}{(\Delta M_K)_{\text{exp}}} \le 0.30\,. \tag{3.7}$$

The search for the oases in question is simplified by the fact that the pair $(\Delta M_s, S_{\psi\phi})$ depends only on $(\tilde{s}_{23}, \delta_2)$, while the pair $(\Delta M_d, S_{\psi K_S})$ only on $(\tilde{s}_{13}, \delta_1)$. The result of this search is similar to the one found in figures 5 and 6 in [14] but the oases differ in details because of slight changes in input parameters and the reduced allowed range on $S_{\psi\phi}$ by about a factor of three.

Having determined the ranges for the parameters (2.7) we can calculate all the remaining flavour observables of interest. In particular we can eliminate those models listed in table 2 which are not capable of providing a shift in ε'/ε larger than say 4×10^{-4}. To this end we show in figure 1 this shift as a function of ε_K for models M8, M9 and M16 and in figure 2 this shift for the remaining models. On the basis of these results we observe the following:

- Only models M8, M9 and M16 are of interest to us as far as ε'/ε is concerned and in what follows we will concentrate our numerical analysis on these three models.

JHEP03(2016)010

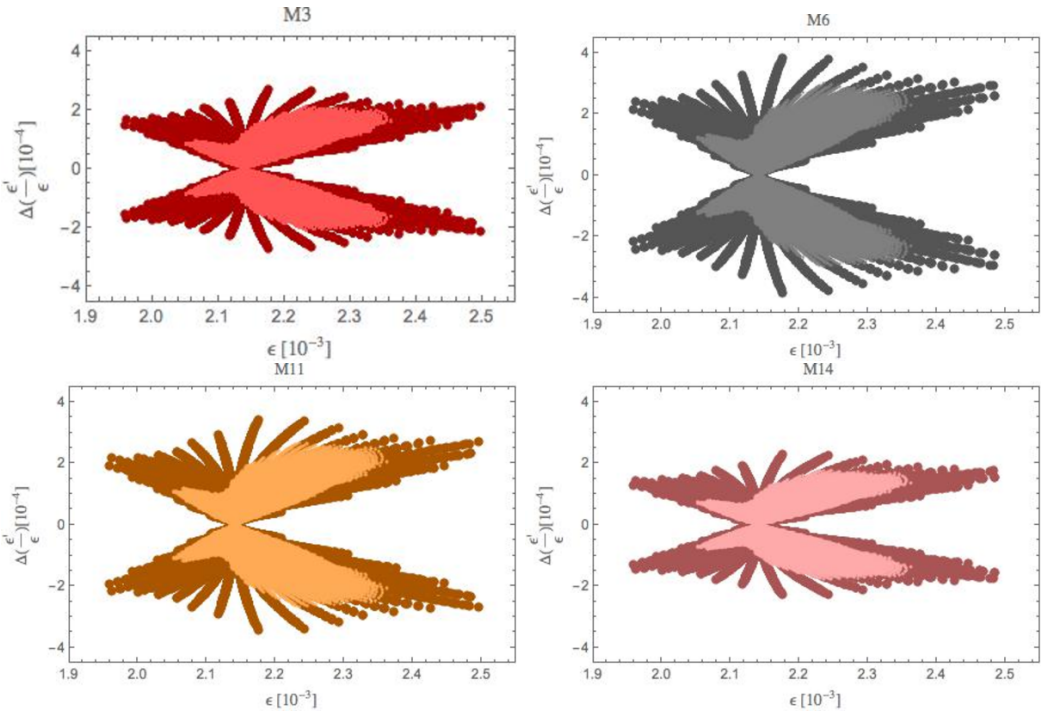

Figure 2. $\Delta(\varepsilon'/\varepsilon)$ versus ε_K for M3, M6, M11 and M14. $M_{Z'} = 3\,\text{TeV}$. Darker regions correspond to present constraints on $\Delta M_{s,d}$ and lighter ones to future projection.

- Interestingly, as mentioned above, the strongest suppression of the rate for $B_s \to \mu^+\mu^-$ can be achieved in M8 and M9 although they have presently difficulties with the LHCb anomalies. Using the formulae in [4] this can be expressed in terms of the relations between the coefficients $C_9^{\rm NP}$ and $C_{10}^{\rm NP}$ which are independent of $M_{Z'}$ and read

$$C_9^{\rm NP} = 0.51\, C_{10}^{\rm NP} \quad \text{(M8)} \qquad C_9^{\rm NP} = 0.42\, C_{10}^{\rm NP} \quad \text{(M9)}\,. \tag{3.8}$$

  They differ significantly from the favourite relations $C_9^{\rm NP} = -C_{10}^{\rm NP}$ or $C_9^{\rm NP} \gg C_{10}^{\rm NP}$ [31, 32].

- On the other hand M16 is the most interesting model for softening the $B_d \to K^*\mu^+\mu^-$ anomaly but cannot help by much in suppressing $B_s \to \mu^+\mu^-$. One finds in this case

$$C_9^{\rm NP} = -4.61\, C_{10}^{\rm NP} \quad \text{(M16)} \tag{3.9}$$

  which is much closer to one of the favourite solutions in which NP resides dominantly in the coefficient C_9.

- Thus already on the basis of B physics observables we should be able to distinguish between (M8,M9) and M16. But the common feature of the three models is that they provide a bigger shift in ε'/ε when the SM value of ε_K is below the data and a positive shift in ε_K is required. This is in particular seen in the case of lighter colours describing decreased uncertainties in $\Delta M_{s,d}$.

JHEP03(2016)010

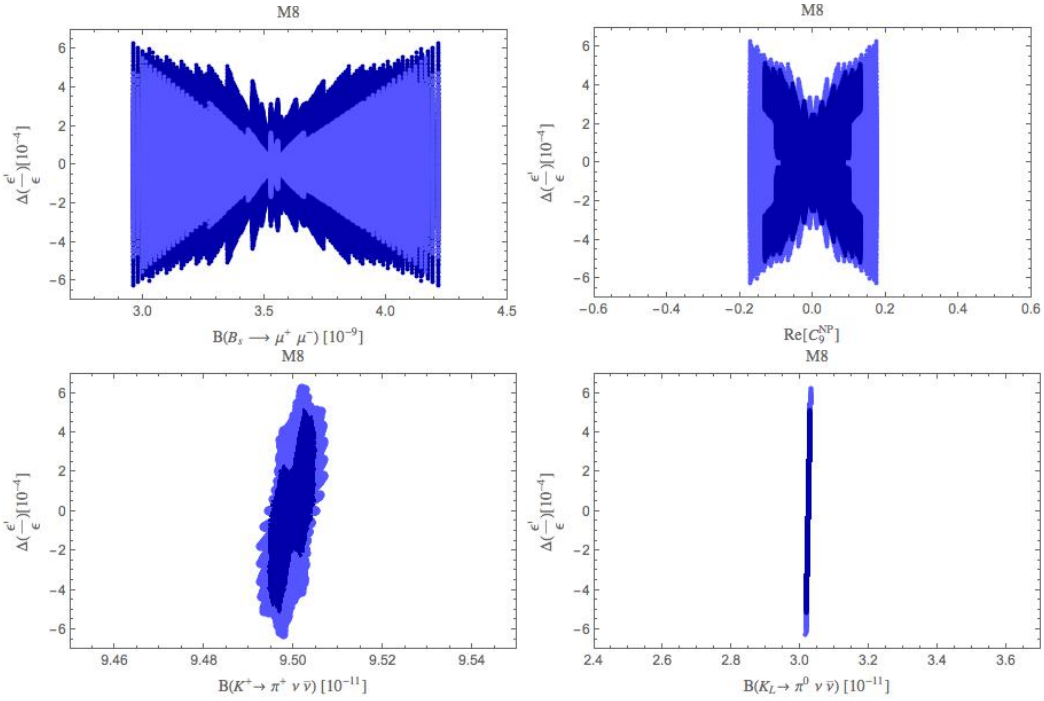

Figure 3. Correlations of $\Delta(\varepsilon'/\varepsilon)$ with various observables for M8 at $M_{Z'} = 3\,\mathrm{TeV}$. Colour coding as in figure 1.

- Most importantly positive shifts in ε'/ε in the ballpark of 6×10^{-4} are possible in these three models, but they are somewhat reduced when the allowed range for $\Delta M_{s,d}$ is reduced. Such shifts could be in principle sufficient to describe the data for ε'/ε.

The question then arises whether the models M8 and M9 while enhancing ε'/ε can simultaneously suppress the rate for $B_s \to \mu^+\mu^-$ and whether M16 while enhancing ε'/ε can simultaneously suppress $\mathrm{Re}C_9$. Moreover correlation of $\Delta(\varepsilon'/\varepsilon)$ with the branching ratios for $K^+ \to \pi^+\nu\bar{\nu}$ and $K_L \to \pi^0\nu\bar{\nu}$ is of great interest in view of NA62 and KOPIO experiments.

In order to answer these questions we used the formulae for $B_{s,d} \to \mu^+\mu^-$, C_9, $K^+ \to \pi^+\nu\bar{\nu}$ and $K_L \to \pi^0\nu\bar{\nu}$ presented in [4] together with the formulae for ε'/ε collected in the previous section to calculate for M8, M9 and M16 models correlation of $\Delta(\varepsilon'/\varepsilon)$ with $\mathcal{B}(B_s \to \mu^+\mu^-)$, $\mathrm{Re}C_9^{\mathrm{NP}}$, $\mathcal{B}(K^+ \to \pi^+\nu\bar{\nu})$ and $\mathcal{B}(K_L \to \pi^0\nu\bar{\nu})$. The result is shown in figures 3, 4 and 5, respectively.

We observe:

- Models M8 and M9 have similar pattern of deviations from the SM with NP effects only relevant in ε'/ε and $B_s \to \mu^+\mu^-$ and in fact positive shift of ε'/ε up to 6×10^{-4} and simultaneous suppression of the rate for $B_s \to \mu^+\mu^-$ up to $(15-20)\%$ are possible in both models. NP effects in C_9, $K^+ \to \pi^+\nu\bar{\nu}$ and $K_L \to \pi^0\nu\bar{\nu}$ are very small.

- In M16 NP effects are only relevant in ε'/ε, C_9 and $K_L \to \pi^0\nu\bar{\nu}$. A positive shift of ε'/ε up to 5×10^{-4} and simultaneous negative shift of C_9 up to -0.55 is possible in this model. But then the rate for $K_L \to \pi^0\nu\bar{\nu}$ is predicted to be suppressed by 15% and the one for $K^+ \to \pi^+\nu\bar{\nu}$ by roughly 5%.

JHEP03(2016)010

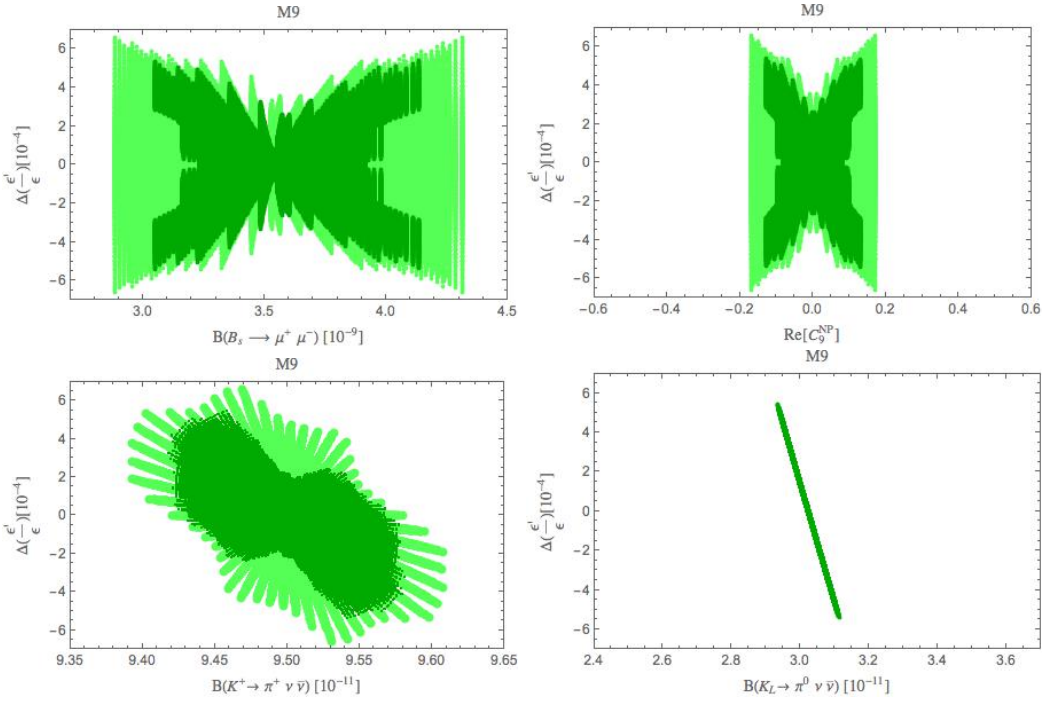

Figure 4. Correlations of $\Delta(\varepsilon'/\varepsilon)$ with various observables for M9 at $M_{Z'} = 3\,\mathrm{TeV}$. Colour coding as in figure 1.

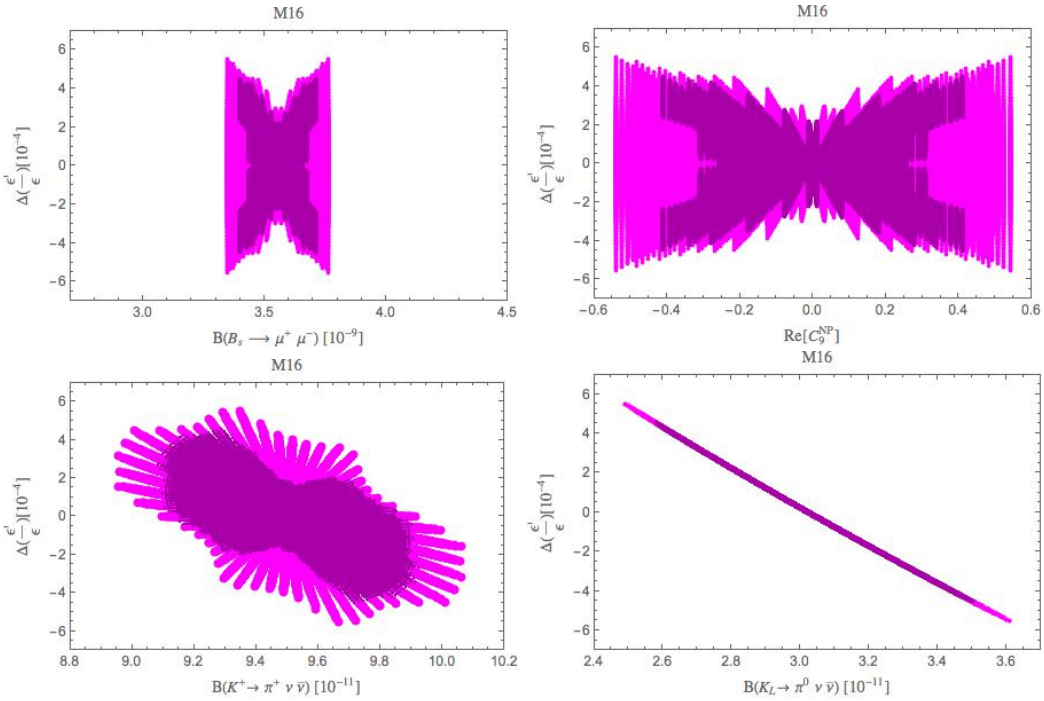

Figure 5. Correlations of $\Delta(\varepsilon'/\varepsilon)$ with various observables for M16 at $M_{Z'} = 3\,\mathrm{TeV}$. Colour coding as in figure 1.

JHEP03(2016)010

$M_{Z'}$	3 TeV	6 TeV	10 TeV	20 TeV	50 TeV	100 TeV
$r_{\varepsilon'}$	1.00	1.08	1.15	1.24	1.36	1.45

Table 4. The $M_{Z'}$ dependence of $r_{\varepsilon'}$.

We conclude therefore that the distinction between M8 and M9 will be very difficult on the basis of observables considered by us but the distinction between these models and M16 should be possible with improved measurements of $B_s \to \mu^+\mu^-$ and improved determination of NP contribution to C_9 which is expected in the flavour precision era. But if NA62 collaboration finds the rate for $K^+ \to \pi^+\nu\bar{\nu}$ significantly above its SM value all these models will fail in describing the data. The same applies to the models in figure 2.

4 Z' outside the reach of the LHC

We will next investigate how the pattern of NP effects changes if $M_{Z'}$ is above 5 TeV and out of the reach of the LHC. As already pointed out in [14], with increased $M_{Z'}$ NP effects in ε_K and ΔM_K increase relative to the ones in $\Delta M_{s,d}$ in 331 models due to particular structure of flavour violating couplings in these models. While the coupling $\Delta_L^{sd}(Z')$ in (2.10) is proportional to the product $\tilde{s}_{13}\tilde{s}_{23}$, the corresponding couplings relevant for $B_{s,d}$ system are given by

$$\Delta_L^{bd}(Z') = \frac{g_2(M_{Z'})}{\sqrt{3}} c_W \sqrt{f(\beta)}\tilde{s}_{13}e^{-i\delta_1}\,, \tag{4.1}$$

$$\Delta_L^{bs}(Z') = \frac{g_2(M_{Z'})}{\sqrt{3}} c_W \sqrt{f(\beta)}\tilde{s}_{23}e^{-i\delta_2}\,, \tag{4.2}$$

each involving only one small parameter $\tilde{s}_{ij}$. ΔM_d and the CP asymmetry $S_{\psi K_S}$ specify the allowed ranges for s_{13} and δ_1, while ΔM_s and the CP asymmetry $S_{\psi\phi}$ specify the allowed ranges for s_{23} and δ_2. In this manner for a given $M_{Z'}$ the allowed ranges of the four parameters entering the K meson system are determined. But, can be further constrained by ε_K and in particular by ΔM_K for sufficiently large $M_{Z'}$ as explained below. We refer to the plots in [14].

In order to proceed we would like to point out that with increasing $M_{Z'}$ the RG analysis leading to (2.11) has to be improved modifying this formula to

$$\left(\frac{\varepsilon'}{\varepsilon}\right)_{Z'} = \pm r_{\varepsilon'} 1.1\,[\beta f(\beta)]\,\tilde{s}_{13}\tilde{s}_{23}\sin(\delta_2-\delta_1)\left[\frac{B_8^{(3/2)}}{0.76}\right]\left[\frac{3\,\text{TeV}}{M_{Z'}}\right]^2 \tag{4.3}$$

with the upper sign for F_1 and the lower for F_2. The parameter $r_{\varepsilon'}$ takes into account additional RG evolution above $\mu = M_{Z'} = 3\,\text{TeV}$ into account and reaches $r_{\varepsilon'} = 1.45$ for $M_{Z'} = 100\,\text{TeV}$. This could turn out to be useful in models in which the $\Delta F = 2$ constraints could be eliminated, for instance in the presence of other operators. But in 331 models this is not possible and as we will see for $M_{Z'} \geq 50\,\text{TeV}$ NP effects in ε'/ε are suppressed in all 331 models. In table 4 we give the values of $r_{\varepsilon'}$ for different $M_{Z'}$.

In order to analyze NP effects beyond the LHC scales we recall the formulae for the shifts due to NP in $\Delta F = 2$ observables.

JHEP03(2016)010

In the K meson system we have

$$(\Delta\varepsilon_K)^{Z'} = 1.76\times 10^4\, r_\varepsilon \left[\frac{3\,\text{TeV}}{M_{Z'}}\right]^2 \text{Im}\left[\Delta_L^{sd}(Z')^*\right]^2 . \tag{4.4}$$

$$\frac{(\Delta M_K)^{Z'}}{(\Delta M_K)_{\text{exp}}} = 5.29\times 10^4\, r_\varepsilon \left[\frac{3\,\text{TeV}}{M_{Z'}}\right]^2 \text{Re}\left[\Delta_L^{sd}(Z')^*\right]^2 , \tag{4.5}$$

where r_ε describes RG effects above $M_{Z'} = 3\,\text{TeV}$. These effects are much smaller than in the case of ε'/ε and in fact suppress slightly NP contribution to ε_K, ΔM_K and also $\Delta M_{s,d}$. But even for $M_{Z'} = 100\,\text{TeV}$ this factor amounts to $r_\varepsilon \approx 0.95$ in the NP contributions to these observables and for $M_{Z'} \le 50\,\text{TeV}$ this effect can be fully neglected. But we keep this factor in formulae below for the future in case various uncertainties decrease.

From (4.3) and (4.4) we find

$$(\Delta\varepsilon_K)^{Z'} = \mp\frac{g^2(M_{Z'})c_W^2}{\beta}\tilde{s}_{13}\tilde{s}_{23}\cos(\delta_2-\delta_1)\left[\frac{r_\varepsilon}{r_{\varepsilon'}}\right]\left[\frac{0.76}{B_8^{(3/2)}}\right] 1.07\times 10^4 \left(\frac{\varepsilon'}{\varepsilon}\right)_{Z'} \tag{4.6}$$

with $-$ for F_1 and $+$ for F_2. From (4.3) and (4.5) we have on the other hand

$$\frac{(\Delta M_K)^{Z'}}{(\Delta M_K)_{\text{exp}}} = \pm\frac{g^2(M_{Z'})c_W^2}{\beta}\tilde{s}_{13}\tilde{s}_{23}\left[\frac{\cos(2(\delta_2-\delta_1))}{\sin(\delta_2-\delta_1)}\right]\left[\frac{r_\varepsilon}{r_{\varepsilon'}}\right]\left[\frac{0.76}{B_8^{(3/2)}}\right] 1.60\times 10^4 \left(\frac{\varepsilon'}{\varepsilon}\right)_{Z'} \tag{4.7}$$

with $+$ for F_1 and $-$ for F_2. The SM contribution to ΔM_K is subject to much larger hadronic uncertainties than is the case of ε_K and it is harder to find out what is the room left for NP contributions. In fact we do not even know the required sign of this contribution. But as we will see soon this constraint could become relevant with improved theory for high values of $M_{Z'}$ and we will impose the constraint in (3.7). For the present discussion we neglect the effects of $Z - Z'$ mixing which will be included in the numerics.

The formula (4.6) represents a correlation between $\Delta M_{s,d}$, $S_{\psi K_S}$ and $S_{\psi\phi}$ which for a given β determine all parameters on its r.h.s. and the ratio of ε'/ε and $(\Delta\varepsilon_K)^{Z'}$. Even if $M_{Z'}$ does not enter explicitly this expression, the allowed values for $\tilde{s}_{13}$ and $\tilde{s}_{23}$ depend on it. Similar comments apply to (4.7).

The relation between the Z' effects in $\Delta F = 2$ master functions S_i are related as follows [14]

$$\frac{\Delta S_K}{\Delta S_d \Delta S_s^*} \propto M_{Z'}^2 \left[\frac{\Delta_L^{sd}(Z')}{\Delta_L^{bd}(Z')\Delta_L^{bs*}(Z')}\right]^2 \propto M_{Z'}^2\,(1-(1+\beta^2)s_W^2). \tag{4.8}$$

Indeed NP contributions to $\Delta M_{s,d}$ are proportional to $\Delta S_{s,d}$ and in ε_K to ΔS_K. This relation follows then from the fact that

$$\Delta S_s \propto \left[\frac{\tilde{s}_{23}}{M_{Z'}}\right]^2, \qquad \Delta S_d \propto \left[\frac{\tilde{s}_{13}}{M_{Z'}}\right]^2. \qquad \Delta S_K \propto \left[\frac{\tilde{s}_{13}\tilde{s}_{23}}{M_{Z'}}\right]^2. \tag{4.9}$$

Presently the strongest constraints on the parameters $\tilde{s}_{ij}$ come from $\Delta F = 2$ processes. With increasing value of $M_{Z'}$ the maximal values of $\tilde{s}_{ij}$ allowed by these constraints increase with increasing $M_{Z'}$. This in turn has impact on the $M_{Z'}$ dependence of maximal values of NP contributions to $\Delta F = 1$ observables that in addition to explicit $M_{Z'}$ dependence through Z' propagator depend sensitively on $\tilde{s}_{ij}$.

JHEP03(2016)010

Now if the $B^0_{s,d} - \bar{B}^0_{s,d}$ mixing constraints dominate, which turns out still the case for $M_{Z'} \leq 30\,\text{TeV}$, one has

$$\tilde{s}^{\max}_{13} \propto M_{Z'}, \qquad \tilde{s}^{\max}_{23} \propto M_{Z'}\,, \qquad (\Delta M_{s,d} \ \text{constraints}), \tag{4.10}$$

where we neglect RG effects. In this case with increasing $M_{Z'}$:

- Maximal NP effects in ε'/ε increase slowly with RG effects represented by $r_{\varepsilon'}$.
- Maximal NP effects in $B_{s,d}$ decays decrease like $1/M_{Z'}$ when their intereference with SM contribution dominates the modifications in the branching ratios.
- Maximal NP effects in $K^+ \to \pi^+\nu\bar{\nu}$ and $K_L \to \pi^0\nu\bar{\nu}$ are independent of $M_{Z'}$.
- Maximal NP effects in ε_K and ΔM_K increase quadratically with $M_{Z'}$ up to the point at which $\tilde{s}_{13}$ and $\tilde{s}_{23}$ reach maximal values allowed by the unitarity of the new mixing matrix. But this point is never reached as in particular ΔM_K constraint becomes important with increasing $M_{Z'}$ much earlier.

As maximal NP contributions to ε_K and ΔM_K allowed by $B^0_{s,d}-\bar{B}^0_{s,d}$ mixing constraints increase fast with increasing $M_{Z'}$ these two observables will dominate the allowed ranges for $\tilde{s}_{ij}$ at sufficiently high value of $M_{Z'}$ and the pattern of $M_{Z'}$ dependences changes. Assuming for simplicity that the maximal values of $\tilde{s}_{13}$ and $\tilde{s}_{23}$ have the same $M_{Z'}$ dependence we have this time at fixed $\delta_2 - \delta_1$

$$\tilde{s}^{\max}_{13} \propto \sqrt{M_{Z'}}, \qquad \tilde{s}^{\max}_{23} \propto \sqrt{M_{Z'}}\,, \qquad (\varepsilon_K,\, \Delta M_K \ \text{constraints}). \tag{4.11}$$

In this case with increasing $M_{Z'}$:

- Maximal NP effects in ε'/ε decrease up to RG effects represented by $r_{\varepsilon'}$ as $1/M_{Z'}$.
- Maximal NP effects in $B_{s,d}$ decays decrease like $1/M^{1.5}_{Z'}$ when the intereference with SM contribution dominates the modifications in the branching ratios.
- Maximal NP effects in $K^+ \to \pi^+\nu\bar{\nu}$ and $K_L \to \pi^0\nu\bar{\nu}$ decrease as $1/M_{Z'}$.
- Maximal NP effects in $\Delta M_{s,d}$ decrease as $1/M_{Z'}$.

A closer inspection of formulae (4.3), (4.6) and (4.7) shows that it is the ΔM_K constraint that is most important. Indeed, in order to have NP in ε'/ε to be significant, we need $\sin(\delta_2 - \delta_1) \approx \pm 1$ with the sign dependent on the model considered as listed in the last column in table 2. This is allowed by $B^0_{s,d} - \bar{B}^0_{s,d}$ mixing constraints. But then as seen in (4.6) the shift in ε_K can be kept small in the presence of a significant shift in ε'/ε by having $\cos(\delta_2 - \delta_1)$ very small. However, in the case of ΔM_K this is not possible as in this limit (4.7) reduces to

$$\frac{(\Delta M_K)^{Z'}}{(\Delta M_K)_{\text{exp}}} = \mp \frac{g^2(M_{Z'})c_W^2}{\beta}\tilde{s}_{13}\tilde{s}_{23}\sin(\delta_2 - \delta_1)\left[\frac{r_\varepsilon}{r_{\varepsilon'}}\right]\left[\frac{0.76}{B_8^{(3/2)}}\right] 1.49 \times 10^4 \left(\frac{\varepsilon'}{\varepsilon}\right)_{Z'} \tag{4.12}$$

with $-$ for F_1 and and $+$ for F_2. From the signs of β and $\sin(\delta_2-\delta_1)$ in table 2 we find therefore that for large values of $M_{Z'}$ significant enhancement of ε'/ε in 331 models implies uniquely suppression of ΔM_K for all 331 models considered and for sufficiently large values of $M_{Z'}$ this suppression will be too large to agree with data and this in turn will imply suppression of ε'/ε. This suppression of ΔM_K is not accidental and is valid in any Z' model in which flavour violating couplings of Z' to quarks are dominantly imaginary as one can easily derive from (4.5). For $\sin(\delta_2-\delta_1)\approx\pm1$ as required in 331 models to get large shift in ε'/ε the relevant couplings must indeed be dominantly imaginary but in general Z' models this could not necessarily be the case and also enhancements of ΔM_K could be possible.

When $\Delta M_{s,d}$, ε_K and ΔM_K constraints are equally important the pattern is more involved but these dependences indicate what we should roughly expect. The main message from this analysis is that with increasing $M_{Z'}$ the importance of NP effects in K meson system is likely to increase relative to the one in $B_{s,d}$ systems. But one should be cautioned that this depends also on other parameters and on the size of departures of SM predictions for various observables from the data.

Therefore, a detailed quantitative analysis of this pattern will only be possible when the room left for NP in the quantities in question will be better known. But, the message is clear: possible tensions in ε'/ε and ε_K can be removed in 331 models for values of $M_{Z'}$ beyond the LHC easier than in rare $B_{s,d}$ decays.

As an example we show in figure 6 $\Delta(\varepsilon'/\varepsilon)$ versus ε_K for the favourite models M8, M9 and M16 at $M_{Z'}=10\,\text{TeV}$. We observe in accordance with our arguments that at this mass the maximal effects in ε'/ε found at $M_{Z'}=3\,\text{TeV}$ are still possible and the range for possible values of ε_K is significant increased. NP contributions to ΔM_K at these scales at $M_{Z'}=10\,\text{TeV}$ are still at most of $\pm4\%$ and the ΔM_K constraint begins to play a role only for $M_{Z'}\geq30\,\text{TeV}$.

In figure 7 we show the correlation of $\Delta(\varepsilon'/\varepsilon)$ with $B_s\to\mu^+\mu^-$ for $M_{Z'}=10\,\text{TeV}$ in models M8 and M9 and the correlations of $\Delta(\varepsilon'/\varepsilon)$ with C_9 and $K_L\to\pi^0\nu\bar{\nu}$ in M16. To this end we imposed the constraints in (3.4), (3.5) and (3.7). As expected from $M_{Z'}$ dependences discussed above, we observe that when the $B^0_{s,d}-\bar{B}^0_{s,d}$ mixing constraints still dominate, NP effects in $B_s\to\mu^+\mu^-$ and C_9 are significantly decreased while they remain practically unchanged in the case of ε'/ε and $K_L\to\pi^0\nu\bar{\nu}$.

With further increase of $M_{Z'}$ NP effects in $B_s\to\mu^+\mu^-$ and C_9 further decrease but the maximal effects in $K_L\to\pi^0\nu\bar{\nu}$ are unchanged. In ε'/ε they even increase due to the increase of $r_{\varepsilon'}$ so that for $M_{Z'}\approx30\,\text{TeV}$ the shift in ε'/ε can reach approximately 8×10^{-4} in all three models. But for higher values of $M_{Z'}$ the ΔM_K constraint becomes important and NP effects in both ε'/ε and $K_L\to\pi^0\nu\bar{\nu}$ are suppressed relative to the region $M_{Z'}\leq30\,\text{TeV}$ as expected from our discussion of the $M_{Z'}$ dependence. We illustrate this in the case of M16 in figure 8 for $M_{Z'}=50\,\text{TeV}$. The suppression is slightly stronger in the case of $K_L\to\pi^0\nu\bar{\nu}$ because in the case of ε'/ε it is compansated by roughly 10% by the increase of $r_{\varepsilon'}$. The result for the first correlation in M8 and M9 is similar but NP effects in $K_L\to\pi^0\nu\bar{\nu}$ are tiny in these models.

JHEP03(2016)010

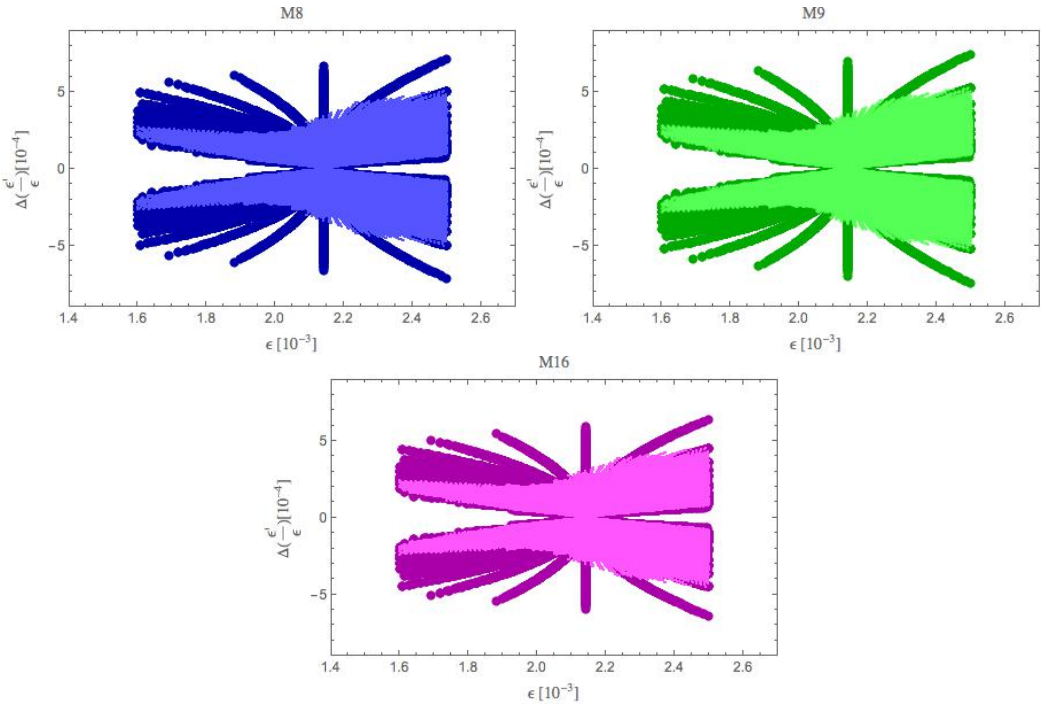

Figure 6. $\Delta(\varepsilon'/\varepsilon)$ versus ε_K for M8, M9 and M16. $M_{Z'} = 10\,\text{TeV}$. Darker regions correspond to present constraints on $\Delta M_{s,d}$ and lighter ones to future projection.

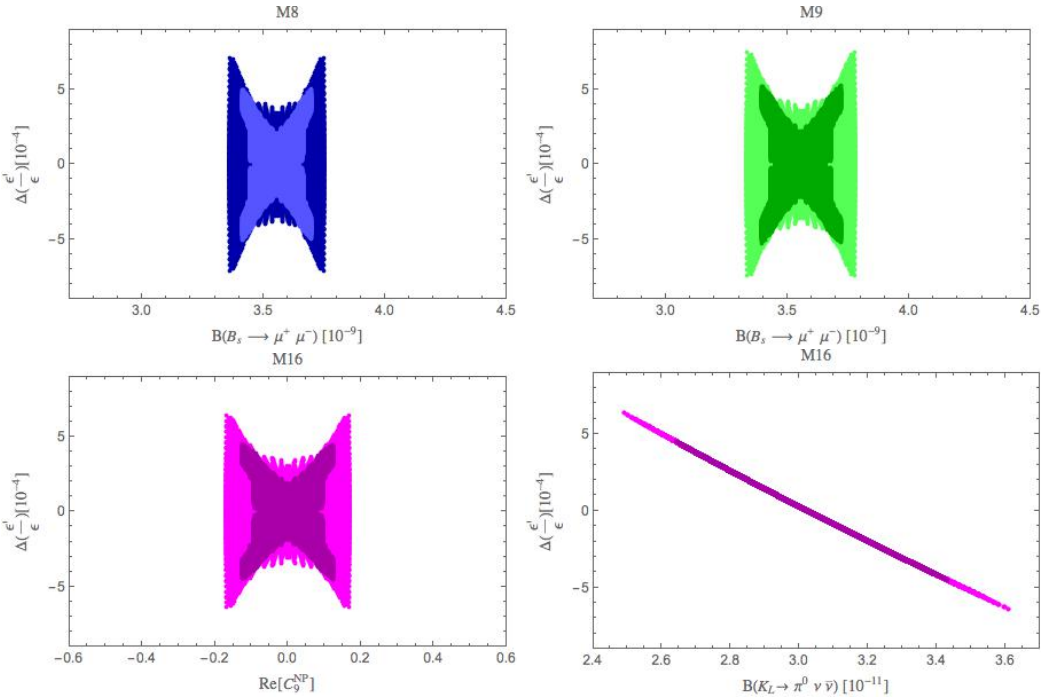

Figure 7. Correlations of $\Delta(\varepsilon'/\varepsilon)$ with various observables for M8, M9 and M16 at $M_{Z'} = 10\,\text{TeV}$. Colour coding as in figure 1.

JHEP03(2016)010

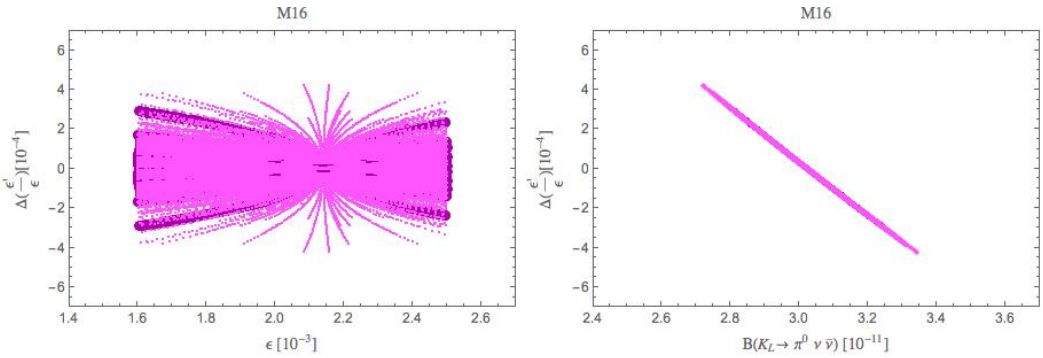

Figure 8. Correlations of $\Delta(\varepsilon'/\varepsilon)$ with ε_K and $K_L \to \pi^0\nu\bar{\nu}$ in M16 at $M_{Z'} = 50\,\text{TeV}$. Colour coding as in figure 1.

5 Summary

In this paper we have updated and improved our analysis of ε'/ε in 331 models presented in [4]. The new analysis has been motivated by the new results for this ratio from [1, 7, 8, 12] which show that ε'/ε within the SM is significantly below the data.

Considering first seven 331 models selected by us in [4] by electroweak precision tests and requiring a shift $\Delta(\varepsilon'/\varepsilon) \geq 4.0 \times 10^{-4}$ by NP, we reduced the number of 331 models to three: M8, M9 and M16 in the terminology of [4]. All three can provide for $M_{Z'} = 3\,\text{TeV}$ a shift in ε'/ε of $(5-6)\cdot 10^{-3}$ and this could in principle be sufficient to bring the theory to agree with data if $B_6^{(1/2)}$ increases towards its upper bound in the future. Moreover:

- Models M8 and M9 can simultaneously suppress $B_s \to \mu^+\mu^-$ but do not offer the explanation of the suppression of the Wilson coefficient C_9 in $B \to K^*\mu^+\mu^-$ (the so-called LHCb anomaly).

- On the contrary M16 offers an explanation of this anomaly simultaneously enhancing ε'/ε but does not provide suppression of $B_s \to \mu^+\mu^-$ which could be required when the data improves and the inclusive value of $|V_{cb}|$ will be favoured.

- NP effects in $K^+ \to \pi^+\nu\bar{\nu}$, $K_L \to \pi^0\nu\bar{\nu}$ and $B \to K(K^*)\nu\bar{\nu}$ are small which can be regarded as prediction of these models to be confronted in the future with NA62, KOPIO and Belle II results.

- Interestingly for values of $M_{Z'}$ well above the LHC scales our favourite 331 models can still successfully face the ε'/ε anomaly and also possible tensions in ε_K can easier be removed than for $M_{Z'}$ in the reach of the LHC. This is clearly seen in figure 6 obtained for $M_{Z'} = 10\,\text{TeV}$ and similar behaviour is found for $M_{Z'}$ up to 30 TeV with maximal NP contribution to ε'/ε increased by RG effects up to 8×10^{-4}. On the other hand, as seen in figure 7, the effects in $B_s \to \mu^+\mu^-$ and C_9 are found above $M_{Z'} = 10\,\text{TeV}$ to be very small. For $M_{Z'} = 50\,\text{TeV}$ also effects in ε'/ε become too small to be able to explain the ε'/ε anomaly.

JHEP03(2016)010

The possibility of accessing masses of $M_{Z'}$ far beyond the LHC reach in 331 models with the help of ε'/ε and ε_K is very appealing but one should keep in mind that the future of 331 models will crucially depend on the improved theory for ε'/ε and $\Delta F = 2$ observables and improved data on rare $B_{s,d}$ and K decays as we have stressed at various places of this writing, in particular when presenting numerous plots.

Acknowledgments

We thank Christoph Bobeth for discussions. This research was done and financed in the context of the ERC Advanced Grant project "FLAVOUR"(267104) and was partially supported by the DFG cluster of excellence "Origin and Structure of the Universe".

References

[1] A.J. Buras, M. Gorbahn, S. Jäger and M. Jamin, *Improved anatomy of ε'/ε in the Standard Model*, *JHEP* **11** (2015) 202 [arXiv:1507.06345] [INSPIRE].

[2] F. Pisano and V. Pleitez, *An* SU(3) × U(1) *model for electroweak interactions*, *Phys. Rev.* **D 46** (1992) 410 [hep-ph/9206242] [INSPIRE].

[3] P.H. Frampton, *Chiral dilepton model and the flavor question*, *Phys. Rev. Lett.* **69** (1992) 2889 [INSPIRE].

[4] A.J. Buras, F. De Fazio and J. Girrbach-Noe, *Z-Z' mixing and Z-mediated FCNCs in* $\mathrm{SU}(3)_C \times \mathrm{SU}(3)_L \times \mathrm{U}(1)_X$ *models*, *JHEP* **08** (2014) 039 [arXiv:1405.3850] [INSPIRE].

[5] M. Blanke, A.J. Buras and S. Recksiegel, *Quark flavour observables in the Littlest Higgs model with T-parity after LHC Run 1*, arXiv:1507.06316 [INSPIRE].

[6] A.J. Buras, D. Buttazzo and R. Knegjens, $K \to \pi\nu\overline{\nu}$ *and* ϵ'/ϵ *in simplified new physics models*, *JHEP* **11** (2015) 166 [arXiv:1507.08672] [INSPIRE].

[7] T. Blum et al., $K \to \pi\pi$ $\Delta I = 3/2$ *decay amplitude in the continuum limit*, *Phys. Rev.* **D 91** (2015) 074502 [arXiv:1502.00263] [INSPIRE].

[8] RBC, UKQCD collaborations, Z. Bai et al., *Standard Model Prediction for Direct CP-violation in* $K \to \pi\pi$ *Decay*, *Phys. Rev. Lett.* **115** (2015) 212001 [arXiv:1505.07863] [INSPIRE].

[9] NA48 collaboration, J.R. Batley et al., *A Precision measurement of direct CP-violation in the decay of neutral kaons into two pions*, *Phys. Lett.* **B 544** (2002) 97 [hep-ex/0208009] [INSPIRE].

[10] KTeV collaboration, A. Alavi-Harati et al., *Measurements of direct CP-violation, CPT symmetry and other parameters in the neutral kaon system*, *Phys. Rev.* **D 67** (2003) 012005 [*Erratum ibid.* **D 70** (2004) 079904] [hep-ex/0208007] [INSPIRE].

[11] KTeV collaboration, E. Abouzaid et al., *Precise Measurements of Direct CP-violation, CPT Symmetry and Other Parameters in the Neutral Kaon System*, *Phys. Rev.* **D 83** (2011) 092001 [arXiv:1011.0127] [INSPIRE].

JHEP03(2016)010

[12] A.J. Buras and J.-M. Gérard, *Upper bounds on ε'/ε parameters $B_6^{(1/2)}$ and $B_8^{(3/2)}$ from large-N QCD and other news*, *JHEP* **12** (2015) 008 [arXiv:1507.06326] [INSPIRE].

[13] A.J. Buras, D. Buttazzo, J. Girrbach-Noe and R. Knegjens, *$K^+ \to \pi^+\nu\overline{\nu}$ and $K_L \to \pi^0\nu\overline{\nu}$ in the Standard Model: status and perspectives*, *JHEP* **11** (2015) 033 [arXiv:1503.02693] [INSPIRE].

[14] A.J. Buras, F. De Fazio, J. Girrbach and M.V. Carlucci, *The Anatomy of Quark Flavour Observables in 331 Models in the Flavour Precision Era*, *JHEP* **02** (2013) 023 [arXiv:1211.1237] [INSPIRE].

[15] A.J. Buras, F. De Fazio and J. Girrbach, *331 models facing new $b \to s\mu^+\mu^-$ data*, *JHEP* **02** (2014) 112 [arXiv:1311.6729] [INSPIRE].

[16] R.A. Diaz, R. Martinez and F. Ochoa, *$\mathrm{SU}(3)_c \times \mathrm{SU}(3)_L \times \mathrm{U}(1)_X$ models for β arbitrary and families with mirror fermions*, *Phys. Rev.* **D 72** (2005) 035018 [hep-ph/0411263] [INSPIRE].

[17] A.E. Carcamo Hernandez, R. Martinez and F. Ochoa, *Z and Z' decays with and without FCNC in 331 models*, *Phys. Rev.* **D 73** (2006) 035007 [hep-ph/0510421] [INSPIRE].

[18] Particle Data Group collaboration, K.A. Olive et al., *Review of Particle Physics*, *Chin. Phys.* **C 38** (2014) 090001 [INSPIRE].

[19] S. Aoki et al., *Review of lattice results concerning low-energy particle physics*, *Eur. Phys. J.* **C 74** (2014) 2890 [arXiv:1310.8555] [INSPIRE].

[20] A.J. Buras, F. De Fazio and J. Girrbach, *$\Delta I = 1/2$ rule, ε'/ε and $K \to \pi\nu\bar{\nu}$ in $Z'(Z)$ and G' models with FCNC quark couplings*, *Eur. Phys. J.* **C 74** (2014) 2950 [arXiv:1404.3824] [INSPIRE].

[21] HPQCD collaboration, I. Allison et al., *High-Precision Charm-Quark Mass from Current-Current Correlators in Lattice and Continuum QCD*, *Phys. Rev.* **D 78** (2008) 054513 [arXiv:0805.2999] [INSPIRE].

[22] A.J. Buras, M. Jamin and P.H. Weisz, *Leading and Next-to-leading QCD Corrections to ϵ Parameter and $B^0 - \bar{B}^0$ Mixing in the Presence of a Heavy Top Quark*, *Nucl. Phys.* **B 347** (1990) 491 [INSPIRE].

[23] J. Urban, F. Krauss, U. Jentschura and G. Soff, *Next-to-leading order QCD corrections for the $B^0 - \bar{B}^0$ mixing with an extended Higgs sector*, *Nucl. Phys.* **B 523** (1998) 40 [hep-ph/9710245] [INSPIRE].

[24] Heavy Flavor Averaging Group (HFAG) collaboration, Y. Amhis et al., *Averages of b-hadron, c-hadron and τ-lepton properties as of summer 2014*, arXiv:1412.7515 [INSPIRE].

[25] A.J. Buras, J.-M. Gérard and W.A. Bardeen, *Large-N Approach to Kaon Decays and Mixing 28 Years Later: $\Delta I = 1/2$ Rule, $\hat{B}_K$ and ΔM_K*, *Eur. Phys. J.* **C 74** (2014) 2871 [arXiv:1401.1385] [INSPIRE].

[26] A.J. Buras and D. Guadagnoli, *Correlations among new CP-violating effects in $\Delta F = 2$ observables*, *Phys. Rev.* **D 78** (2008) 033005 [arXiv:0805.3887] [INSPIRE].

[27] A.J. Buras, D. Guadagnoli and G. Isidori, *On ϵ_K Beyond Lowest Order in the Operator Product Expansion*, *Phys. Lett.* **B 688** (2010) 309 [arXiv:1002.3612] [INSPIRE].

[28] J. Brod and M. Gorbahn, *Next-to-Next-to-Leading-Order Charm-Quark Contribution to the CP-violation Parameter ε_K and ΔM_K*, *Phys. Rev. Lett.* **108** (2012) 121801 [arXiv:1108.2036] [INSPIRE].

JHEP03(2016)010

[29] J. Brod and M. Gorbahn, ϵ_K *at Next-to-Next-to-Leading Order: The Charm-Top-Quark Contribution*, *Phys. Rev.* **D 82** (2010) 094026 [arXiv:1007.0684] [INSPIRE].

[30] CKMFITTER GROUP collaboration, K. Trabelsi, *World average and experimental overview of* γ/φ_3, presented at *The 8th International Workshop on the CKM Unitarity Triangle*, Vienna University of Technology, Vienna, Austria, 8–12 September 2014, ckmfitter.in2p3.fr.

[31] W. Altmannshofer and D.M. Straub, *New physics in* $b \to s$ *transitions after LHC run 1*, *Eur. Phys. J.* **C 75** (2015) 382 [arXiv:1411.3161] [INSPIRE].

[32] S. Descotes-Genon, L. Hofer, J. Matias and J. Virto, *Global analysis of* $b \to s\ell\ell$ *anomalies*, arXiv:1510.04239 [INSPIRE].

JHEP03(2016)010